

Subtropical ocean ecosystem structure changes forced by North Pacific climate variations

ROBERT R. BIDIGARE^{1*}, FEI CHAI², MICHAEL R. LANDRY³, ROGER LUKAS⁴, CECELIA C. S. HANNIDES⁴, STEPHANIE J. CHRISTENSEN⁴, DAVID M. KARL⁴, LEI SHI² AND YI CHAO⁵

¹HAWAII INSTITUTE OF MARINE BIOLOGY, UNIVERSITY OF HAWAII, PO BOX 1346, KANEHOE, HI 96744, USA, ²SCHOOL OF MARINE SCIENCES, UNIVERSITY OF MAINE, 5706 AUBERT HALL, ORONO, ME 04469, USA, ³SCRIPPS INSTITUTION OF OCEANOGRAPHY, UNIVERSITY OF CALIFORNIA, 9500 GILMAN DRIVE, LA JOLLA, CA 92093, USA, ⁴DEPARTMENT OF OCEANOGRAPHY, UNIVERSITY OF HAWAII, 1000 POPE ROAD, HONOLULU, HI 96822, USA AND ⁵JET PROPULSION LABORATORY, 4800 OAK GROVE DRIVE, PASADENA, CA 91109, USA

*CORRESPONDING AUTHOR: bidigare@hawaii.edu

Received April 1, 2009; accepted in principle June 30, 2009; accepted for publication July 5, 2009; published online 31 July, 2009

Corresponding editor: William Li

Biological responses to basin-scale climate forcing in the subtropical North Pacific Ocean are assessed based on temporal variations in plankton community structure observed at Station ALOHA and results of a coupled physical–biogeochemical model. Observational data and model simulations for the period 1990–2004 reveal distinct temporal patterns, with significant increases in net primary productivity, modeled nitrate flux into the euphotic zone and the measured downward flux of particulate nitrogen during 1999–2004. Concurrent increases in microalgae, cyanobacteria and modeled and measured zooplankton biomass were also observed during this period. We provide evidence that these responses were a consequence of climate forcing that destratified the upper ocean, making it more susceptible to mixing events and nutrient entrainment. These findings underscore the importance of nitrate flux and plankton community structure, as modulated by climate forcing, in regulating particle export over interannual and decadal time scales.

INTRODUCTION

The U.S. Global Ocean Flux Study (GOFS) initiated time-series measurement programs near Hawaii (Hawaii Ocean Time-series, HOT) and Bermuda (Bermuda Atlantic Time-series Study, BATS) in 1988 (Karl and Michaels, 1996). The primary objectives of these programs are to resolve physical and biogeochemical variability at the seasonal and interannual time scales and to provide observational data for developing and evaluating biogeochemical models. While interannual trends in mesozooplankton biomass and phytoplankton pigments have been reported for the HOT site (Sakamoto *et al.*, 2004; Sheridan and Landry, 2004), interpretation of patterns of variability has proven challenging due to the one-dimensional nature of the time-series data sets. Here we combine field observations

with the output of a coupled physical–biogeochemical ocean model to provide insight into mechanisms responsible for temporal variations in plankton community structure and particle export in the subtropical North Pacific Ocean. The synthesis presented here extends the “bottom-up” interpretations of Corno *et al.* (Corno *et al.*, 2007) by including zooplankton data (top-down control) and a biogeochemical modeling component. The latter was included in response to the insightful theory developed by Thingstad (Thingstad, 1998): “To understand the behavior of an ecosystem with a high degree of regenerated production, there is a need for a tool by which mechanisms of growth and loss, of nutrient uptake and nutrient recycling, of bottom-up and top-down control, can be integrated into one picture.”

METHOD

Data source

In situ observations (temperature and salinity profiles, pigment concentrations, picophytoplankton abundances, daytime mesozooplankton biomass (>0.2 mm), primary production rates and particulate nitrogen fluxes) were made as part of the NSF-funded HOT program at Station ALOHA (22°45'N, 158°W). Mesozooplankton dry weight biomass values were converted to units of mmol N m⁻² using the equations derived for this region (Landry *et al.*, 2001). These data sets, as well as methodological details and other core measurement data, can be found at: <http://hahana.soest.hawaii.edu/hotcold.html>.

Numerical models

The physical model is based on the Regional Ocean Modeling System (ROMS), which has been configured for the Pacific Ocean (45°S to 65°N, 99°E to 70°W) at 50-km resolution (Wang and Chao, 2004). There are 20 levels in the vertical axis. The biogeochemical model is based on the Carbon, Si(OH)₄, Nitrogen Ecosystem (CoSINE) model (Chai *et al.*, 2002). The CoSINE model includes silicate, nitrate and ammonium, two phytoplankton groups, two grazers and two detrital pools. Below the euphotic zone, sinking particulate organic matter is converted to inorganic nutrients by a regeneration process similar to the one used by Chai *et al.* (1996), in which organic matter decays to ammonium and then is nitrified to nitrate. The CoSINE model has been used in studies of decadal variability in primary production of the North Pacific (Chai *et al.*, 2003) and nutrient and pCO₂ distributions in the equatorial Pacific (Jiang and Chai, 2005).

Recently, the CoSINE model has been coupled with ROMS for the Pacific basin-scale configuration. The Pacific basin-scale ROMS–CoSINE model output has been analyzed for nutrient transport and its impact on biological productivity on seasonal and interannual time scales in the South China Sea (Liu and Chai, 2009). Chai *et al.* (in press) used the same model output to compare the modeled air–sea CO₂ flux with the observed values, and investigated the controlling factors for the air–sea CO₂ flux in the South China Sea. Polovina *et al.* (2008a, b) analyzed the ROMS–CoSINE model output around the northern atolls in the Hawaiian Archipelago during the period 1964–2006. The ROMS–CoSINE showed considerable interannual and decadal variation in productivity, and changes in

recent years that were coherent with observed changes at higher trophic levels (Polovina *et al.*, 2008a, b).

Initialized with climatological temperature, salinity, nutrients (WOA 2001, http://www.nodc.noaa.gov/OC5/WOA01/pr_woa01.html) and TCO₂ (Key *et al.*, 2004), the Pacific ROMS–CoSINE model has been forced with the climatological air–sea fluxes calculated using the bulk formula for several decades in order to reach quasi-equilibrium. The ROMS–CoSINE model is then integrated during 1955–2005, forced with daily air–sea fluxes of momentum, heat and fresh-water derived from the NCEP/NCAR reanalysis (Kalnay *et al.*, 1996). Surface wind stress is calculated from the 10-m wind and a drag coefficient formulation (Large and Pond, 1982). Heat flux is calculated from the prescribed short- and long-wave radiations, sensible and latent heat fluxes calculated by the bulk formula with prescribed air temperature and relative humidity. Fresh-water flux is derived from the prescribed precipitation, and evaporation is derived from the latent heat flux from the sea surface. Model results depend upon the quality of surface forcing (wind, heat and fresh water fluxes); interannual and decadal variations in the surface forcing generate changes of ocean circulation and hydrographic conditions. Previous circulation modeling efforts that have used different surface forcing products for the Pacific Ocean tend to produce similar conclusions regarding interannual and decadal variability (Xie *et al.*, 2000). The ROMS–CoSINE simulated plankton biomass, nutrient fluxes and salinity anomalies are used in this analysis.

Climate indices

Variations in measured and modeled atmospheric, physical and biogeochemical variables were examined in relation to the phases of the Pacific Decadal Oscillation (PDO), El Niño–Southern Oscillation (ENSO) and the North Pacific Index (NPI). We included the latter two indices based on a previous study that concluded “a single indicator such as the PDO is incomplete in characterizing North Pacific climate” (Bond *et al.*, 2003). Monthly mean anomalies of the Pacific Decadal Oscillation (PDO) were generously provided by N. Mantua (<http://jisao.washington.edu/pdo/>). ENSO evolution was depicted using the NINO3.4 index, where NINO3.4 is the average sea surface temperature anomaly in the area bounded by 5°N to 5°S and 170°W to 120°W; monthly values were obtained from the NOAA Climate Prediction Center (CPC) website <http://www.cpc.ncep.noaa.gov/data/indices/>. The NPI from the CPC represents a measure of the anomalous atmospheric circulation over the North Pacific from

Table I: Summary of annual time-series data for 1990–1997 (HP, Huber’s parameter used for regime shift detection and N/A time-series data not available)

Variable	HP	1990	1991	1992	1993	1994	1995	1996	1997
North Pacific Index (NPI) anomaly	1	0.33	0.20	1.33	1.53	0.23	0.53	0.30	1.05
Σ Fucoxanthin (0–200 m, mg m ⁻²) ^a	2	10.69	9.76	8.95	8.28	8.14	7.93	9.57	10.54
19′-hexanoyloxyfucoxanthin (0–200 m, mg m ⁻²)	2	5.00	4.82	4.39	4.17	4.60	4.51	5.41	5.78
19′-butanoyloxyfucoxanthin (0–200 m, mg m ⁻²)	2	4.15	3.64	3.29	3.02	2.83	2.67	3.32	3.42
Zeaxanthin (0–200 m, mg m ⁻²) ^b	2	7.41	7.48	7.67	6.29	6.33	6.24	7.88	8.86
Photosynthetic nanoeukaryotes (0–200 m, 10 ⁻¹¹ cells m ⁻²)	2	N/A	0.93	1.43	1.35	1.17	1.20	1.30	2.09
Modeled nitrate flux at 175 m (mmol m ⁻² day ⁻¹)	2	0.35	0.38	0.23	0.17	0.11	0.11	0.07	0.23
Measured particulate N flux at 150 m (mmol N m ⁻² day ⁻¹)	2	0.37	0.31	0.22	0.23	0.25	0.22	0.23	0.29
Net primary production rate (0–200 m, mmol C m ⁻² day ⁻¹)	2	29.99	43.60	44.77	37.57	36.16	43.66	39.85	36.41
Modeled zooplankton biomass (0–200 m, mmol N m ⁻²)	1	4.78	3.83	3.47	2.85	2.55	2.15	2.27	2.57
Measured daytime zooplankton (0–160 m, mmol N m ⁻²)	1	N/A	N/A	N/A	N/A	3.12	3.01	3.84	3.14

^a Σ Fucoxanthin is a biomass proxy for chromophyte microalgae, including diatoms (fucoxanthin), prymnesiophytes (19′-hexanoyloxyfucoxanthin) and pelagophytes (19′-butanoyloxyfucoxanthin).

^b Zeaxanthin is a biomass proxy for cyanobacteria, primarily *Prochlorococcus* spp. (see text for details).

Table II: Summary of annual time-series data for 1998–2004

Variable	HP	1998	1999	2000	2001	2002	2003	2004
North Pacific Index (NPI) anomaly	1	-1.73	-0.73	-0.40	-0.63	-0.18	-0.40	-0.60
Σ Fucoxanthin (0–200 m, mg m ⁻²)	2	12.51	12.11	13.28	11.93	13.03	11.81	16.00
19′-hexanoyloxyfucoxanthin (0–200 m, mg m ⁻²)	2	7.33	6.98	7.33	6.92	7.50	6.76	9.25
19′-butanoyloxyfucoxanthin (0–200 m, mg m ⁻²)	2	3.96	4.08	3.98	4.01	4.47	3.77	4.93
Zeaxanthin (0–200 m, mg m ⁻²)	2	10.08	10.61	9.79	10.85	10.42	10.41	13.64
Photosynthetic nanoeukaryotes (0–200 m, 10 ⁻¹¹ cells m ⁻²)	2	1.51	1.33	1.46	1.60	1.72	2.32	2.23
Modeled nitrate flux at 175 m (mmol m ⁻² day ⁻¹)	2	0.28	0.36	0.62	0.23	0.31	0.45	0.65
Measured particulate N flux at 150 m (mmol N m ⁻² day ⁻¹)	2	0.31	0.34	0.30	0.36	0.32	0.39	0.29
Net primary production rate (0–200 m, mmol C m ⁻² day ⁻¹)	2	42.10	45.07	48.70	47.74	50.69	47.77	43.62
Modeled zooplankton biomass (0–200 m, mmol N m ⁻²)	1	2.22	6.73	7.45	4.91	5.05	5.18	6.08
Measured daytime zooplankton (0–160 m, mmol N m ⁻²)	1	4.08	3.79	4.26	5.81	4.92	5.13	5.15

spring into summer. Annual values of the NPI were obtained from the NOAA Bering Climate website: <http://www.beringclimate.noaa.gov/>.

Statistical analyses

Statistical analysis of geophysical time-series data is confounded by “red noise” (i.e. serial correlation). To avoid potential bias, regime shifts were identified using the Shift Detection software (version 3-2) developed by (Rodionov, 2004, 2006). All analyses used the original data with AR1 correction, a probability of 0.2, a cutoff length of 10 years and the IP4 red noise estimation algorithm. A variable Huber’s weight parameter was used to adjust for outliers (Tables I and II). Huber’s (Huber, 2005) weight parameter was calculated as $\text{weight} = \min(1, \text{parameter}/(|\text{anomaly}|))$, where anomaly is the deviation from the expected mean value of the new regime normalized by the standard deviation averaged for all consecutive sections of the cutoff length in the series (Rodionov, 2006). This software is available at <http://www.beringclimate.noaa.gov/regimes/>.

RESULTS AND DISCUSSION

To evaluate the basin-wide model performance, we compare the modeled sea surface height (SSH) anomaly with the satellite-derived SSH anomaly. We normalize the satellite SSH anomaly by its standard deviation, and then perform the empirical orthogonal function (EOF) analysis. The first mode of the EOF of the normalized satellite SSH anomaly (Fig. 1A) shows an out-of-phase relationship between the eastern tropical Pacific (ETP) and the North Pacific Ocean. The coastal regions off the US west coast from California to Alaska are in phase with the ETP signal. This is consistent with the sea surface temperature patterns associated with the PDO (Mantua *et al.*, 1997). Using the same procedure, we normalize the modeled SSH anomaly with its standard deviation and perform the EOF analysis (Fig. 1B). The physical model captures the characteristic spatial patterns of the SSH signal as well as the sharp transition around 1997–1998 (Fig. 1C). Between 1990 and 1997, the ETP had anomalously high SSH, whereas SSH in the North Pacific subtropical gyre was unusually low. During 1998, this SSH mode switched

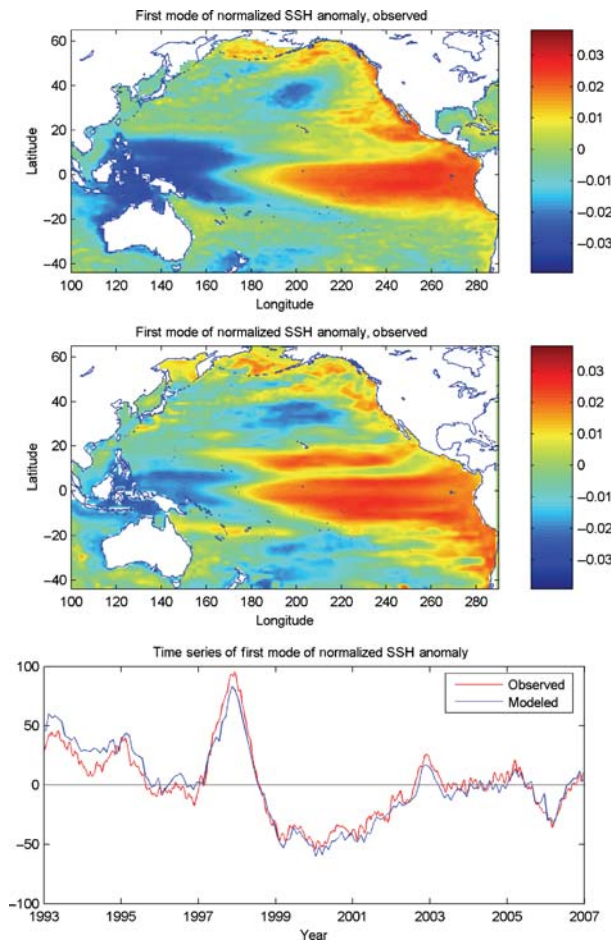


Fig. 1. Spatial patterns of the first mode of the empirical orthogonal function (EOF) derived from (A) normalized sea surface height (SSH) from altimeter satellite observations (dimensionless) and (B) normalized SSH ROMS simulations (dimensionless), (C) the associated time-series (dimensionless), showing the magnitude in percentage relative to the standard deviation of the original data. The seasonal cycle was removed before performing the EOF analysis.

sign, with a lower SSH in the ETP and higher SSH in the North Pacific Current.

Maximum positive PDO and NINO3.4 anomalies are observed during late 1997 and early 1998, a period coincident with a shift in North Pacific Index (NPI) anomalies from positive to negative values (Fig. 2A and B) and with the mature phase of the strong warm 1997–1998 El Niño–Southern Oscillation (ENSO) event. NPI values during 1990–1997 were significantly higher than those during 1998–2004 (Table III). For the purpose of comparing upper ocean properties at Station ALOHA (0–200 m) before and after the NPI sign change, we partitioned temperature and salinity measurements into two time periods, 1990–1997 and 1998–2004, even though some effects of the transition at ALOHA may be delayed. Comparison of potential temperature–salinity

(T–S) plots during these intervals reveals changes in water mass characteristics at Station ALOHA (Fig. 2C). The increase in measured (and modeled) salinity during 1998–2004 is most apparent in the upper 160 m of the water column (Fig. 3), which includes the top of the nitracline (~100 m) and most of the euphotic zone (0–175 m). The salinity increase in the mixed layer has been ascribed to a regional decrease in the net flux of freshwater (Lukas, 2001). Subsurface salinity anomalies on isopycnals that are below the mixed layer (i.e. part of the thermocline) primarily reflect subduction and subsequent along-isopycnal advection of anomalously salty surface waters (Lukas and Santiago-Mandujano, 2008). The upper pycnocline salinity anomalies exhibit a dominant decadal cycle, which is associated with rainfall anomalies in the region north of Hawaii where these isopycnals are ventilated (Lukas and Santiago-Mandujano, 2008). Reduced stratification of the upper water column was a consequence of the mixed-layer salinity increase, and an associated decrease in temperature. We hypothesize that the post-1998 destratification of the upper ocean, in combination with (wind) mixing events, contributed to the 2-fold increase in the modeled flux of nitrate into the euphotic zone (Table III).

Increase in the availability of new nitrogen, primarily in the form of nitrate, is the likely explanation for the observed enhancement of microalgal biomass and net primary productivity during 1999–2004 (Fig. 2E; Table III). High-performance liquid chromatography (HPLC) pigment analyses document a 40% increase in the concentrations of Σ fucoxanthin (fucoxanthin and its acyloxy derivatives 19'-hexanoyloxyfucoxanthin and 19'-butanoyloxyfucoxanthin) during the last half of this 15-year time-series (Fig. 4A; Table III). The maximum increase is at 80–140 m, while concentrations in the upper 40 m are low and relatively constant throughout the entire period. These carotenoid pigments are associated with certain members of the chromophyte microalgae, including diatoms, prymnesiophytes and pelagophytes. This finding is consistent with the 45% increase in abundance of photosynthetic eukaryotes, dominated by small cells of 3–4 μm or less, as measured by flow cytometry (Table III). It should be noted that these observations are in apparent conflict with ocean color satellite imagery that suggests a decrease in surface chlorophyll concentrations in the subtropical Pacific Ocean during 1999–2004 (Gregg *et al.*, 2005; Behrenfeld *et al.*, 2006; Polovina *et al.*, 2008a, b). This disparity is likely due to the fact that ocean color satellite imagery only measures near surface phytoplankton pigment biomass, while the largest biomass increases are observed below the remote sensing depth (~25 m) at Station ALOHA.

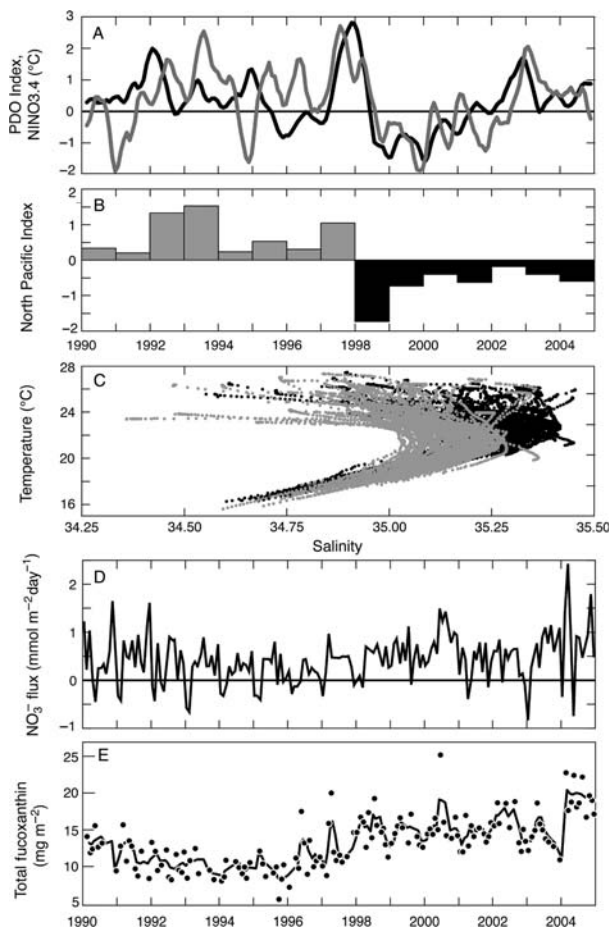


Fig. 2. Temporal variations in climatological indices, hydrographic properties and atmospheric forcing during 1990–2004: (A) PDO (grey line, three-point running average) and NINO3.2 (black line, three-point running average) indices, (B) yearly means of the North Pacific Index during 1990–1997 (grey bars) and 1998–2004 (black bars), (C) potential temperature (θ)–salinity (T–S) plots for the upper 200 db at Station ALOHA during 1990–1997 (grey dots) and 1998–2004 (black dots), (D) modeled nitrate flux into the euphotic zone ($\text{mmol N m}^{-2} \text{ day}^{-1}$) and (E) integrated chromophyte microalgae pigment (0–200 db, mg m^{-2} , black line corresponds to the three-point running average; cf. Table III) computed for the Station ALOHA region.

After 1998, HPLC analyses of pigment samples from the upper 120 m also showed a significant increase in zeaxanthin (Table III; Fig. 4B), the biomarker for cyanobacteria, a diverse group of oxygenic phototrophic prokaryotes, including *Prochlorococcus* and *Synechococcus*, as well as the nitrogen-fixers, *Trichodesmium* and *Crocospaera*. Among cyanobacteria, *Prochlorococcus* spp. are unique in containing the pigment α -carotene instead of β -carotene (Chisholm *et al.*, 1988). Thus, a strong correlation between depth-integrated (0–200 m) concentrations of α -carotene and zeaxanthin over the 1994–2004 study period ($R^2 = 0.76$, $n = 113$) suggests that the observed increase in zeaxanthin at Station ALOHA

was primarily due to *Prochlorococcus* spp. Since the zeaxanthin content scales as a function of biovolume for *Prochlorococcus* and *Synechococcus* (Moore *et al.*, 1995), the observed increase in zeaxanthin at Station ALOHA likely corresponds to biomass enhancement rather than photo-adaptation.

The Carbon, Si(OH)₄, Nitrogen Ecosystem (CoSINE) biogeochemical model simulation predicted a relatively constant phytoplankton biomass during 1990–2004 ($24.18 \pm 0.23 \text{ mmol N m}^{-2}$, 1% coefficient of variation, $n = 15$). This was a consequence of the predicted increase in total zooplankton biomass of 45% ($2.96 \text{ mmol N m}^{-2}$ during 1990–1998 vs. $5.90 \text{ mmol N m}^{-2}$ during 1999–2004), which maintained the modeled phytoplankton biomass at relatively constant levels during the 15-year time-series (Table III). This prediction is supported by the observation that measured mesozooplankton biomass during 1999–2004 ($4.84 \text{ mmol N m}^{-2}$) was 41% higher than that measured during 1994–1998 ($3.44 \text{ mmol N m}^{-2}$) (Fig. 4; Tables I and II). It is likely that the zooplankton dynamics at Station ALOHA were responsible for the $\sim 25\%$ increase in the downward flux of particulate nitrogen (PN) at 150 m during the latter half of this time-series (Fig. 4C–E). Measured PN flux ($0.27 \text{ mmol N m}^{-2} \text{ day}^{-1}$) was significantly higher than the rate of nitrate flux at the base of the euphotic zone ($0.22 \text{ mmol N m}^{-2} \text{ day}^{-1}$) during 1990–1998 ($P = 0.054$, $n = 9$, two-tailed paired *t*-test). Presumably, the excess PN flux ($0.05 \text{ mmol N m}^{-2} \text{ day}^{-1}$) measured during 1990–1998 is a consequence of nitrogen fixation (Karl *et al.*, 1997). By comparison, recent $\delta^{15}\text{N}$ determinations of nitrate and particulate nitrogen during June–July 2004 yielded a nitrogen fixation rate of $0.045 \text{ mmol N m}^{-2} \text{ day}^{-1}$ at Station ALOHA (Casciotti *et al.*, 2008). While the average rate of nitrate flux ($0.44 \text{ mmol N m}^{-2} \text{ day}^{-1}$) was $0.10 \text{ mmol N m}^{-2} \text{ day}^{-1}$ higher than the rate of PN flux ($0.34 \text{ mmol N m}^{-2} \text{ day}^{-1}$) during 1999–2004, these values are not statistically different ($P = 0.261$, $n = 6$, two-tailed paired *t*-test). Since the rates of nitrate and PN flux are roughly in balance during this period, the new production associated with nitrogen fixation was presumably accumulated as dissolved organic nitrogen in the euphotic zone and/or transferred to higher tropic levels via zooplankton grazing (Church *et al.*, 2002; Hannides, 2007).

SYNTHESIS

While direct field observations and the ROMS–CoSINE model utilized in this study both have inherent limitations, their combination provides new insights into

Table III: Summary of regime shifts detected for atmospheric, physical, chemical and biological variables during 1990–2004

Variable	Year shift detected (<i>P</i>)	Mean before shift (length, years)	Mean after shift (length, years)	B/A
North Pacific Index (NPI) anomaly	1998 (0.001)	0.69 (8)	−0.64 (7)	−
Modeled nitrate flux at 175 m (mmol m ^{−2} day ^{−1})	1999 (0.132)	0.22 (9)	0.44 (6)	2.00
Net primary production rate (0–200 m, mmol C m ^{−2} day ^{−1})	1999 (0.003)	39.35 (9)	47.27 (6)	1.20
19′-hexanoxyfucoxanthin (0–200 m, mg m ^{−2})	1998 (0.011)	4.84 (8)	7.44 (7)	1.54
19′-butanoxyfucoxanthin (0–200 m, mg m ^{−2})	1998 (0.181)	3.29 (8)	4.17 (7)	1.27
Σ Fucoxanthin (0–200 m, mg m ^{−2})	1998 (0.100)	9.23 (8)	12.95 (7)	1.40
Photosynthetic nanoeukaryotes (0–200 m, 10 ^{−11} cells m ^{−2})	1997 (0.023)	1.23 (7)	1.78 (8)	1.45
Zeaxanthin (0–200 m, mg m ^{−2})	1998 (0.087)	7.27 (8)	10.83 (7)	1.49
Modeled zooplankton biomass (0–200 m, mmol N m ^{−2})	1999 (0.046)	2.96 (9)	5.90 (6)	1.99
Measured daytime zooplankton (0–160 m, mmol N m ^{−2})	2001 (0.026)	3.61 (7)	5.25 (4)	1.45
Measured PN flux (150 m, mmol N m ^{−2} day ^{−1})	1999 (0.050)	0.27 (9)	0.34 (6)	1.24

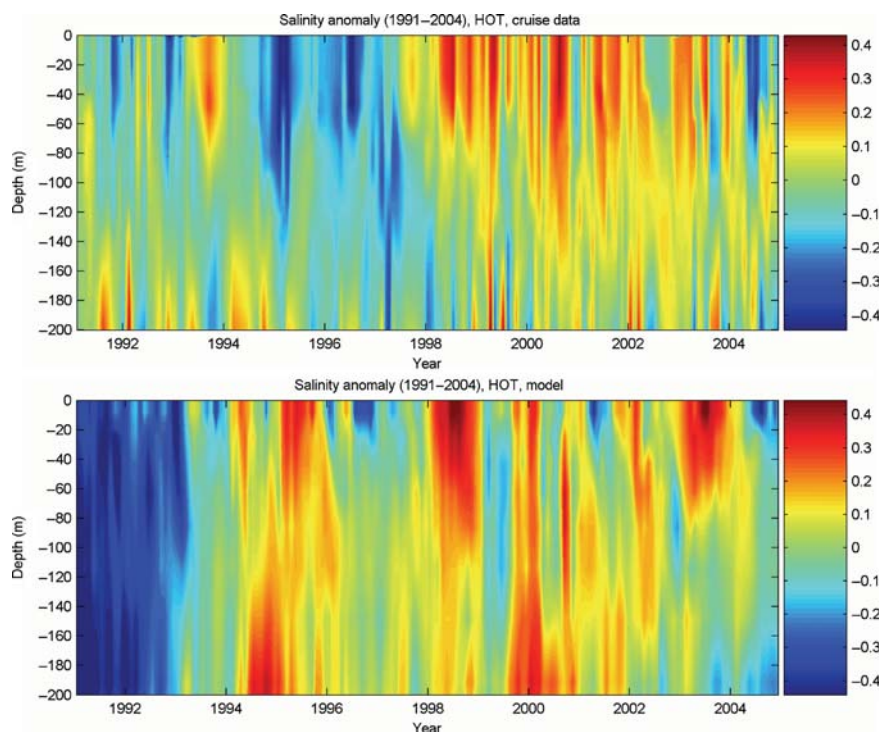


Fig. 3. Temporal variations in the measured (top panel) and modeled (bottom panel) salinity anomaly in the upper 200 db at Station ALOHA during 1991–2004.

the complex nature of climate and marine ecosystem interactions in the North Pacific subtropical gyre. We suggest that the atmospheric changes associated with the rapid transition from positive values of the PDO and ENSO to sustained negative values during 1998 set into motion a cascade of events that include an increase in net freshwater flux from the ocean and the appearance of anomalously high salinity waters at Station ALOHA (Figs 2C and 3). As a consequence, the upper ocean became more weakly stratified and susceptible to mixing events forced by winds. The increase in upper-ocean mixing from 1998 onward enhanced the

biological utilization of new nitrate nitrogen (Dugdale and Goering, 1967; Eppley and Peterson, 1979; Benitez-Nelson *et al.*, 2007), increasing the biomass of photosynthetic eukaryotes (small pennate diatoms, prymnesiophytes and pelagophytes). This process is consistent with the proposed mechanism for maintaining a net autotrophic state in the subtropical North Pacific Ocean (Karl *et al.*, 2003; Riser and Johnson, 2008). Since *Prochlorococcus* is not capable of nitrate utilization (Moore *et al.*, 2002), regeneration of phytoplankton nitrogen to ammonium via remineralization processes likely served as the nutrient source for the observed

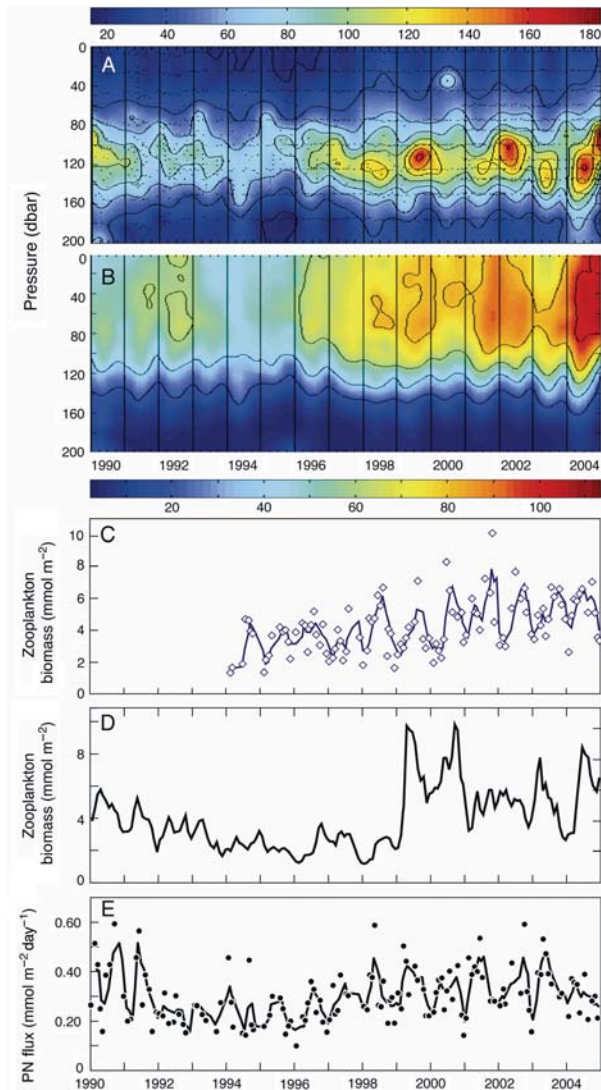


Fig. 4. Temporal variations in biological parameters at Station ALOHA during 1990–2004: **(A)** contours of chromophyte microalgae pigment concentrations in the upper 200 db ($\mu\text{g m}^{-3}$, cf. Table III), **(B)** contours of zeaxanthin concentrations in the upper 200 db ($\mu\text{g m}^{-3}$), **(C)** measured daytime mesozooplankton biomass (0–160 m, mmol N m^{-2} , black line corresponds to the three-point running average), **(D)** modeled zooplankton biomass (0–200 m, mmol N m^{-2}) and **(E)** measured flux of particulate nitrogen (PN) at 150 m ($\text{mmol N m}^{-2} \text{day}^{-1}$, black line corresponds to the three-point running average) at Station ALOHA.

increase in *Prochlorococcus* biomass, with an implied connection to enhanced microzooplankton grazing activity (Fig. 5). It should be noted that a similar cascade of events was recently reported by Li and Harrison (Li and Harrison, 2008) for the Bedford Basin (Canada) during the period of 1994–2006. The enhanced eukaryotic phytoplankton biomass (and growth), in turn, increased the carrying capacity of this subtropical ecosystem for higher trophic levels including the

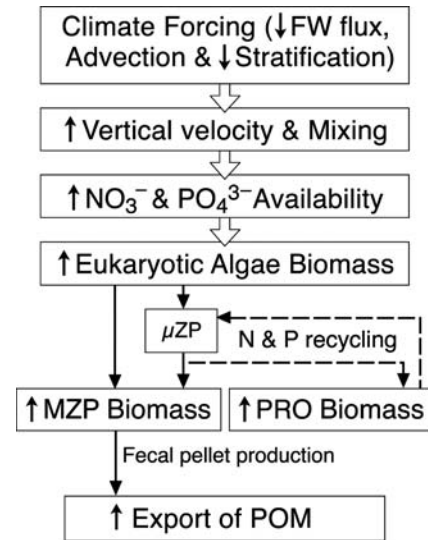


Fig. 5. Conceptual model depicting influences of remote and local forcings on physical and biogeochemical parameters at Station ALOHA (\uparrow , increase; \downarrow , decrease; N , NH_4^+ ; P , PO_4^{3-} ; μZP , microzooplankton; MZP, mesozooplankton; PRO, *Prochlorococcus* spp.; POM, particulate organic matter).

mesozooplankton. The coherence in the temporal patterns of nitrate flux, total fucoxanthin, measured mesozooplankton biomass and PN flux lead us to conclude that temporal variations in nitrate flux and plankton community, as modulated by climate forcing, are important in regulating the export of particulate organic matter export over interannual and decadal time scales. Future studies are needed to quantify the influences of submesoscale and mesoscale variability and passing storms on upper ocean biogeochemistry in the subtropical North Pacific Ocean.

ACKNOWLEDGEMENTS

The HOT program data sets summarized herein would not exist without the dedicated and skilled efforts of a large cadre of scientists and technicians, including R. Letelier, K. Björkman, J. Christian, J. Dore, L. Fujieki, D. Hebel, T. Houlihan, P. Lethaby, U. Maggaard, D. Sadler, F. Santiago-Mandujano, J. Snyder, L. Tupas and C. Winn. We are also grateful to M. Latasa and M. Ondrusek who helped with the HPLC pigment analyses.

FUNDING

This research was supported by grants from the National Science Foundation (EF-04245999 awarded to D.M.K.; OCE-0326616 awarded to D.M.K. and

R.R.B.; OCE-0117919 and OCE-0327513 awarded to R.L., OCE-0324666 awarded to M.R.L; and EF-0424599 awarded to D.M.K. and R.R.B), the National Aeronautics and Space Administration, the Environmental Protection Agency, the Gordon and Betty Moore Foundation and by the State of Hawaii.

REFERENCES

- Behrenfeld, M. J., O'Malley, R. T., Siegel, D. A. *et al.* (2006) Climate-driven trends in contemporary ocean productivity. *Nature*, **444**, 752–755.
- Benitez-Nelson, C. R., Bidigare, R. R., Dickey, T. D. *et al.* (2007) Mesoscale eddies drive increased silica export in the subtropical Pacific Ocean. *Science*, **316**, 1017–1021.
- Bond, N. A., Overland, J. E., Spillane, M. *et al.* (2003) Recent shifts in the state of the North Pacific. *Geophys. Res. Lett.*, **30**, 2183. doi:10.1029/2003GL018597.
- Casciotti, K. L., Glover, D. M., Trull, T. *et al.* (2008) Constraints on nitrogen cycling at the subtropical North Pacific station ALOHA from isotopic measurements of nitrate and particulate nitrogen. *Deep-Sea Res. II*, **55**, 1661–1672.
- Chai, F., Barber, R. T. and Lindley, S. T. (1996) Origin and maintenance of high nutrient condition in the equatorial Pacific. *Deep-Sea Res. II*, **42**, 1031–1064.
- Chai, F., Dugdale, R. C., Peng, T.-H. *et al.* (2002) One dimensional ecosystem model of the equatorial Pacific upwelling system, Part I: model development and silicon and nitrogen cycle. *Deep-Sea Res. II*, **49**, 2713–2745.
- Chai, F., Jiang, M., Barber, R. T. *et al.* (2003) Interdecadal variation of the transition zone chlorophyll front, a physical-biological model simulation between 1960 and 1990. *J. Oceanogr.*, **59**, 461–475.
- Chai, F., Liu, G., Xue, H. *et al.* (2009) Seasonal and interannual variability of carbon cycle in South China Sea: a three dimensional physical-biogeochemical modeling study. *J. Oceanogr.* in press.
- Chisholm, S. W., Olson, R. J., Zettler, E. R. *et al.* (1988) A novel free-living prochlorophyte abundant in the oceanic euphotic zone. *Nature*, **334**, 340–343.
- Church, M. J., Ducklow, H. W. and Karl, D. M. (2002) Multiyear increases in dissolved organic matter inventories at Station ALOHA in the North Pacific Subtropical Gyre. *Limnol. Oceanogr.*, **47**, 1–10.
- Corno, G., Karl, D. M., Church, M. J. *et al.* (2007) The impact of climate forcing on ecosystem processes in the North Pacific Subtropical Gyre. *J. Geophys. Res.*, **112**, C04021. doi:10.1029/2006JC003730.
- Dugdale, R. C. and Goering, J. J. (1967) Uptake of new and regenerated forms of nitrogen in primary productivity. *Limnol. Oceanogr.*, **12**, 196–206.
- Eppley, R. W. and Peterson, B. J. (1979) Particulate organic matter flux and planktonic new production in the deep ocean. *Nature*, **282**, 677–680.
- Gregg, W. W., Casey, N. W. and McClain, C. R. (2005) Recent trends in global ocean chlorophyll. *Geophys. Res. Lett.*, **32**, L03606. doi:10.1029/2004GL021808.
- Hannides, C. C. S. (2007) The 1998 regime shift in the North Pacific Subtropical Gyre: Evidence from zooplankton biomass, abundance and stable isotope analyses. PhD Dissertation. Department of Oceanography, University of Hawaii.
- Huber, P. J. (2005) Robust estimation of a location parameter. *Ann. Math. Stat.*, **35**, 73–101.
- Jiang, M.-S. and Chai, F. (2005) Physical and biological controls on the latitudinal asymmetry of surface nutrients and $p\text{CO}_2$ in the central and eastern equatorial Pacific. *J. Geophys. Res.*, **110**, C06007. doi:10.1029/2004JC002715.
- Kalnay, E., Kanamitsu, M., Kistler, R. *et al.* (1996) The NCEP/NCAR 40-year reanalysis project. *Bull. Amer. Meteor. Soc.*, **77**, 437–471.
- Karl, D. M. and Michaels, A. F. (1996) The Hawaiian Ocean Time-series (HOT) and Bermuda Atlantic Time-series Study (BATS). *Deep-Sea Res. II*, **43**, 127–128.
- Karl, D. M., Letelier, R., Tupas, L. *et al.* (1997) The role of nitrogen fixation in biogeochemical cycling in the subtropical North Pacific Ocean. *Nature*, **388**, 533–538.
- Karl, D. M., Laws, E. A., Morris, P. *et al.* (2003) Metabolic balance of the open sea. *Nature*, **426**, 32.
- Key, R. M., Kozyr, A., Sabine, C. L. *et al.* (2004) A global ocean carbon climatology: Results from Global Data Analysis Project (GLODAP). *Global Biogeochem. Cycles*, **18**, GB4031. doi:10.1029/2004GB002247.
- Landry, M. R., Al-Mutairi, H., Selph, K. E. *et al.* (2001) Seasonal patterns of mesozooplankton abundance and biomass at Station ALOHA. *Deep-Sea Res. II*, **48**, 2037–2206.
- Large, W. G. and Pond, S. (1982) Sensible and latent heat flux measurements over the ocean. *J. Phys. Oceanogr.*, **12**, 464–482.
- Li, W. K. W. and Harrison, G. (2008) Propagation of an atmospheric climate signal to phytoplankton in a small marine basin. *Limnol. Oceanogr.*, **53**, 1734–1745.
- Liu, G. and Chai, F. (2009) Seasonal and interannual variability of primary and export production in the South China Sea: a three-dimensional physical-biogeochemical model study. *ICES J. Mar. Sci.*, **66**, 420–431.
- Lukas, R. (2001) Freshening of the upper thermocline in the North Pacific subtropical gyre associated with decadal changes in rainfall. *Geophys. Res. Lett.*, **28**, 3485–3488.
- Lukas, R. and Santiago-Mandujano, F. (2008) Interannual to interdecadal salinity variations observed near Hawaii: Local and remote forcing by surface freshwater fluxes. *Oceanography*, **21**, 46–55.
- Mantua, N. J., Hare, S. R., Zhang, Y. *et al.* (1997) A Pacific interdecadal climate oscillation with impacts on salmon production. *Bull. Meteorol. Soc.*, **78**, 1069–1079.
- Moore, L. R., Goericke, G. and Chisholm, S. W. (1995) Comparative physiology of *Synechococcus* and *Prochlorococcus*: Influence of light and temperature on growth, pigments, fluorescence and absorptive properties. *Mar. Ecol. Prog. Ser.*, **116**, 259–275.
- Moore, L. R., Post, A. F., Rocap, G. *et al.* (2002) Utilization of different nitrogen sources by the marine cyanobacteria *Prochlorococcus* and *Synechococcus*. *Limnol. Oceanogr.*, **47**, 989–996.
- Polovina, J. J., Howell, E. A. and Abecassis, M. (2008a) Ocean's least productivity waters expanding. *Geophys. Res. Lett.*, **35**, L03618. doi:10.1029/2007GL031745.
- Polovina, J. J., Chai, F., Howell, E. A. *et al.* (2008b) Ecosystem dynamics at a productivity gradient: a study of the lower trophic dynamics around the northern atolls in the Hawaiian Archipelago. *Prog. Oceanogr.*, **77**, 217–224.

- Riser, S. C. and Johnson, K. S. (2008) Net production of oxygen in the subtropical ocean. *Nature*, **451**, 323–325.
- Rodionov, S. N. (2004) A sequential algorithm for testing climate regime shifts. *Geophys. Res. Lett.*, **31**, L09204. doi:10.1029/2003GL018597.
- Rodionov, S. N. (2006) Use of prewhitening in climate regime shift detection. *Geophys. Res. Lett.*, **33**, L12707. doi:10.1029/2006GL025904.
- Sakamoto, C. M., Karl, D. M., Jannasch, H. W. *et al.* (2004) *In situ* nitrate measured on the HALE ALOHA open ocean mooring: Influence of mesoscale eddies and Rossby waves on nutrient variability and ecosystem response. *J. Geophys. Res.*, **109**, 1–12.
- Sheridan, C. C. and Landry, M. R. (2004) A 9-year increasing trend in mesozooplankton biomass at the Hawaii Ocean Time-series Station ALOHA. *ICES J. Mar. Sci.*, **61**, 457–463.
- Thingstad, T. F. (1998) A theoretical approach to structuring mechanisms in the pelagic food web. *Hydrobiologia*, **363**, 59–72.
- Wang, X. and Chao, Y. (2004) Simulated sea surface salinity variability in the tropical Pacific. *Geophys. Res. Lett.*, **31**, L02302. doi:10.1029/2003GLD18146.
- Xie, S.-P., Kunitani, T., Kubokawa, A. *et al.* (2000) Interdecadal thermocline variability in the North Pacific for 1958–1997: a GCM simulation. *J. Phys. Oceanogr.*, **30**, 2798–2813.